



Published in final edited form as:

J Phys Chem B. 2016 February 11; 120(5): 936–944. doi:10.1021/acs.jpcc.5b12233.

Utility of 5-Cyanotryptophan Fluorescence as a Sensitive Probe of Protein Hydration

Beatrice N. Markiewicz^{1,‡}, Debopreeti Mukherjee^{1,‡}, Thomas Troxler^{1,2,*}, and Feng Gai^{1,2,*}

¹Department of Chemistry, University of Pennsylvania, Philadelphia, PA 19104

²The Ultrafast Optical Processes Laboratory, University of Pennsylvania, Philadelphia, PA 19104

Abstract

Tryptophan (Trp) fluorescence has been widely used to interrogate the structure, dynamics and function of proteins. In particular, it provides a convenient and site-specific means to probe a protein's hydration status and dynamics. Herein, we show that a tryptophan analog, 5-cyanotryptophan (Trp_{CN}), can also be used for this purpose, but with the benefit of enhanced sensitivity to hydration. This conclusion is reached based on measurements of the static and time-resolved fluorescence properties of 5-cyanoindole, Trp_{CN}, and Trp_{CN}-containing peptides in different solvents, which indicate that upon dehydration the fluorescence quantum yield (QY) and lifetime (τ_F) of Trp_{CN} undergo a much greater change in comparison to those of Trp. For example, in H₂O the QY of Trp_{CN} is less than 0.01, which increases to 0.11 in 1,4-dioxane. Consistently, the fluorescence decay kinetics of Trp_{CN} in H₂O are dominated by a 0.4 ns component, whereas in 1,4-dioxane the kinetics are dominated by a 6.0 ns component. The versatile utility of Trp_{CN} as a sensitive fluorescence reporter is further demonstrated in three applications, where we used it (1) to probe the solvent property of a binary mixture consisting of dimethyl sulfoxide and H₂O, (2) to monitor the binding interaction of an antimicrobial peptide with lipid membranes, and (3) to differentiate two differently hydrated environments in a folded protein.

1. INTRODUCTION

Among the naturally occurring fluorescent amino acids, tryptophan (Trp) is the most widely used fluorescent probe of protein structure, function, and dynamics.^{1,2} This is because 1) its fluorescence properties, such as the emission wavelength, Stokes shift and lifetime, depend on local environment,^{1,3,4} 2) its fluorescence can be quenched by various amino acid sidechains^{5–7} as well as other molecules or ions,^{8–12} and 3) it has a relatively high fluorescence quantum yield (QY) (i.e., ~0.14 in water)¹³ and large molar extinction coefficient for transitions to the ¹L_a and ¹L_b excited states, which combined, allows for measurements using dilute protein solutions. While Trp is an exceedingly useful and convenient fluorescence reporter of proteins, it affords, like any other spectroscopic probes,

*Corresponding Author: gai@sas.upenn.edu and ttroxler@sas.upenn.edu.

‡These authors made equal contribution

Supporting Information: Fluorescence decay kinetics of 5CI in D₂O, CD spectra of 2W_{CNP} and MPXW_{CN} in H₂O or DPC micelles, and fluorescence spectra of 2W_{CNP} at different DMSO mole fractions. This material is available free of charge via the Internet at <http://pubs.acs.org>.

certain limitations and/or disadvantages. For example, in practice it is often difficult to quantitatively assess and interpret Trp fluorescence results, as many different mechanisms can contribute to the excited-state decay process of the indole fluorophore in a protein environment.^{14–17} Therefore, much effort has been made to expand and/or improve the utility of Trp fluorescence by exploring the feasibility of using various Trp-based non-natural amino acids, such as 7-azatryptophan,¹⁸ 5-hydroxytryptophan,¹⁹ 4- or 5-fluorotryptophan,^{20,21} 6- or 7-cyanotryptophan,²² and β -(1-Azulenyl)-L-alanine,²³ that possess different photophysical properties from Trp (e.g., quantum yield, emission wavelength, and fluorescence decay kinetics). Herein, we continue this effort by showing that the fluorescence emission of a nitrile-derivatized Trp analog, 5-cyanotryptophan (Trp_{CN}), can be used as a sensitive probe of the local hydration status of proteins.

From a practical point of view, for many biological applications a good fluorescence probe should exhibit a significant change in its fluorescence spectrum (i.e., intensity, wavelength, or both) when exposed to different environments. This requirement is especially important for examining processes, such as protein folding and interactions, whereby the local surrounding of the fluorophore undergoes a drastic change, for instance, from a hydrated to a dehydrated environment. While Trp fluorescence has been extensively used in these types of applications, the total fluorescence intensity change is rarely more than two-fold. This is due in part to the fact, as shown (Figure 1), that the fluorescence QY of indole is not sensitively dependent on hydration. Of course, one can find special cases where the change is more drastic due to involvement of other quenching mechanisms, such as those arising from specific sidechains.⁶ In comparison, the fluorescence QY of 5-cyanoindole (5CI), the sidechain of Trp_{CN} , exhibits a much stronger sensitivity to interactions with H_2O as shown below. This is supported by the fact that upon changing the solvent from water to 1,4-dioxane, a solvent commonly used to mimic the hydrophobic interior of proteins, the total fluorescence intensity of 5CI is increased by a factor of approximately 23, whereas that of indole only increases by a factor of ~ 1.3 (Figure 1). Furthermore, a previous study by Jennings *et al.*²⁴ demonstrated that the maximum of the fluorescence spectrum of 5CI is shifted from ~ 315 nm in isopentane to ~ 391 nm in H_2O . Thus, taken together, the large Stokes shift and a more significant QY change of 5CI in response to hydration suggests that Trp_{CN} could be a more sensitive protein hydration probe than Trp.

To verify this notion, we carried out steady-state and time-resolved fluorescence measurements on 5CI, Trp_{CN} , and a model tripeptide Gly- Trp_{CN} -Gly (hereafter referred to as $\text{GW}_{\text{CN}}\text{G}$) in different solvents. We found, as expected, that exposure to water results in significant quenching of the Trp_{CN} fluorescence, due to a substantial increase in its excited-state nonradiative decay rate. On the other hand, the fluorescence QY and lifetime of Trp_{CN} , either in the free amino acid form or in a peptide environment, were found to increase, on average, by more than an order of magnitude in aprotic solvents compared to those in H_2O . Combined, we believe that these results support the idea that Trp_{CN} can be used as a sensitive fluorescence probe of the local hydration status of proteins. Further evidence confirming this utility of Trp_{CN} comes from several applications wherein we demonstrated that this non-natural amino acid can be used to 1) detect the preferential accumulation of dimethyl sulfoxide (DMSO) molecules around aromatic sidechains in a disordered peptide,

2) probe the binding of an antimicrobial peptide to lipid membranes, and 3) differentiate the microenvironments of two Trp_{CN} residues in a folded protein.

2. EXPERIMENTAL SECTION

2.1. Materials and Sample Preparation

5-cyanoindole (5CI) at 99% purity was purchased from Acros Organics (Morris Plains, New Jersey), Fmoc-5-cyano-L-tryptophan with a purity of >99% was purchased from RSP amino acids (Shirley, MA), and all other amino acids were purchased from Advanced ChemTech (Louisville, KY). The following solvents (spectroscopic grade) were purchased from Acros Organics: methanol (MeOH), ethanol (EtOH), dimethyl sulfoxide (DMSO), acetonitrile (ACN), 1,4-dioxane, tetrahydrofuran (THF, without the BHT preservative), and 2,2,2-trifluoroethanol (TFE). D₂O was purchased from Cambridge Isotope Laboratories, Inc. (Tewksbury, MA). Dodecylphosphocholine (DPC) was purchased from Avanti Polar Lipids Inc. (Alabaster, Alabama). All materials and solvents were used as received. Deprotection of the Fmoc-5-cyanotryptophan to produce the free Trp_{CN} amino acid (Trp_{CN}-NH₂) and synthesis of all peptides (Gly-Trp_{CN}-Gly-NH₂, TZ2W_{CN}-NH₂, TC2W_{CN}-NH₂, and MPXW_{CN}-NH₂) were achieved by using standard 9-fluorenylmethoxy-carbonyl (Fmoc) solid-state methods on a CEM (Matthews, NC) Liberty Blue automated microwave peptide synthesizer. Peptide purification was done by reverse-phase HPLC (Agilent Technologies 1260 Infinity) with a C18 preparative column (Vydac). The Trp_{CN} amino acid and all peptides were constructed on Rink amide resin and thus contained an amidated C-terminus. The mass of every peptide was verified by either liquid-chromatography mass spectrometry (LC-MS) or matrix-assisted laser desorption/ionization mass spectrometry (MALDI-MS) where appropriate. Samples were freshly prepared before use by directly dissolving the desired compound in the desired solvent, and the final concentration of the solute was approximately 45 μM for static and time-resolved measurements. The UV-Vis spectra (in the region of 250 – 300 nm) of a 5-cyanoindole solution and an indole solution in methanol of equal concentration (determined by weight) are almost identical. Thus, for each sample we used its absorbance and the molar extinction coefficient of Trp at 280 nm ($\epsilon = 5500 \text{ M}^{-1} \text{ cm}^{-1}$) to estimate the solute concentration. Membrane-bound MPXW_{CN} peptide was prepared by solubilizing MPXW_{CN} with DPC in TFE at a 1:70 peptide to lipid ratio. The organic solvent was removed via a nitrogen stream and the left-over film was lyophilized for at least 4 hours to ensure complete solvent removal. Subsequently, the resultant dry film was redissolved in H₂O. The final concentration of the peptide was ~40 μM.

2.2. Static and Time-Resolved Fluorescence Measurements

Static fluorescence measurements were obtained with a Jobin Yvon Horiba Fluorolog 3.10 spectrofluorometer at room temperature in a 1 cm quartz cuvette with a 1.0 nm resolution and an integration time of 1.0 nm/s. For all the static measurements, an excitation wavelength of 280 nm was used. Time-resolved fluorescence measurements were collected on a time-correlated single photon counting (TCSPC) system with a 0.4 cm quartz cuvette at 25 °C. The details of the TCSPC system have been described elsewhere.²⁵ Briefly, a home-built femtosecond Ti:Sapphire oscillator operating at 800 nm and 85 MHz repetition rate was used to generate a 270 nm excitation pulse train in a home-built collinear third harmonic

generator. Repetition rate was reduced to 21 MHz by using an electro-optical pulse picking system (Conoptics Inc.). Emission was collected at magic angle polarization condition and in a 90 degree geometry relative to excitation, selected by a short-wavelength bandpass filter (Semrock FF01-357/44) around 360 nm and a long-pass filter (Semrock FF01-300/LP) with a 300 nm cutoff to better suppress scattered excitation light, and detected with a MCP-PMT detector (Hamamatsu R2809U) and a TCSPC PC-board (Becker and Hickl SPC-730). Fluorescence decays were deconvoluted with the instrument response function (IRF) and fit either to a single- or multi-exponential function in order to minimize χ^2 below an acceptable value (i.e., 1.2) using FLUOFIT (Picoquant GmbH). *N*-acetyl-L-tryptophanamide (NATA) was used as a standard and control, yielding a single exponential decay of 3.0 ns (see Table 1) in accordance with the literature.¹⁴ The optical density of the samples at the excitation wavelength was equal to or below 0.2 for both static and time-resolved measurements. Furthermore, the quantum yield of a given sample (QY_S) was determined using the quantum yield of NATA (QY_R) in H₂O at pH 7.0 as a reference and the following equation,

$$QY_S = QY_R \frac{I_S}{I_R} \frac{A_R}{A_S} \frac{n_S^2}{n_R^2} \quad (1)$$

where I and A represent the integrated area of the fluorescence spectrum and the optical density of the sample at 280 nm, respectively, and n is the refractive index of the solvent used. The subscripts S and R represent sample and reference, respectively. In addition, the value of QY_R was taken as 0.14,² and 1.333 was used for n_R .

3. RESULTS AND DISCUSSION

To assess the feasibility of using Trp_{CN} fluorescence as a reporter of protein local hydration status, we first systematically examined the steady-state fluorescence properties and fluorescence decay kinetics of 5CI, Trp_{CN}, and GW_{CN}G in a series of solvents with different polarities and hydrogen bonding abilities (Table 1). Then, the utility of this fluorescence probe was tested in three different applications, including detection of a specific solute-solvent interaction, peptide-membrane association, and the hydration status of two Trp_{CN} residues located in different environments within a folded mini-protein.

Steady-State Fluorescence Measurements

As shown (Figure 2), both the intensity and maximum wavelength (λ_{\max}) of the fluorescence spectrum of 5CI exhibit a strong dependence on solvent. Qualitatively, the λ_{\max} of 5CI increases with increasing solvent polarity (Table 1), which is in good agreement with the trend previously observed by Jennings *et al.*²⁴ Furthermore, the λ_{\max} of 5CI is red-shifted compared to the fluorescence spectrum of indole, the fluorophore of Trp, obtained in the same solvent. For example, in H₂O the fluorescence spectrum of indole is peaked at ~352 nm, whereas that of 5CI has an emission maximum at ~387 nm. The greater Stokes shift of 5CI can be attributed to the larger change in its dipole moment upon photoexcitation.²⁶ In addition, and perhaps more importantly, in solvents that can form strong hydrogen bonds (H-bonds), such as H₂O and trifluoroethanol (TFE), the fluorescence QY of 5CI exhibits a significant decrease (Figure 2 and Table 1). For example, in 1,4-dioxane the fluorescence QY of 5CI is determined to be ~0.13, which is decreased to ~0.005

in H₂O. In comparison, while indole is a brighter fluorophore, its fluorescence QY has less of a dependence on these solvents (i.e., 0.45 in 1,4-dioxane versus 0.28 in H₂O).²⁷ Thus, these results indicate that, when used to probe a hydration/dehydration event, 5CI would be able to produce a fluorescence signal with a higher contrast than that of indole.

As shown (Figure 2), the fluorescence spectra of the free amino acid Trp_{CN} are similar to those of 5CI obtained in the same solvents, although the λ_{max} value in each case is further red-shifted (Table 1). This is consistent with the trend already observed for indole and Trp.²⁸ What is more important, however, is that the strong fluorescence quenching effect of H₂O toward the 5CI fluorophore is maintained (Table 1). This result, which is consistent with a previous study,²⁹ indicates that Trp_{CN} fluorescence could be used to sense the local hydration status of proteins. Results obtained with GW_{CN}G (Figure 2 and Table 1), also corroborate this notion. For example, the fluorescence QY of Trp_{CN} and GW_{CN}G is increased by more than an order of magnitude upon changing the solvent from H₂O to MeOH. Since MeOH is also capable of forming hydrogen bonds, this finding thus manifests the specific and high sensitivity of Trp_{CN} fluorescence towards H₂O.

Time-Resolved Measurements

To further understand the photophysics of Trp_{CN}, we set out to measure the fluorescence decay kinetics of 5CI, Trp_{CN}, and GW_{CN}G in those aforementioned solvents. As indicated (Figure 3 and Table 1), the fluorescence decay kinetics of 5CI in all solvents could be fit reasonably well to a single-exponential function, with the exception of those obtained in H₂O and TFE, which required at least a double-exponential function to yield a satisfactory fitting (i.e., $\chi^2 < 1.2$). Consistent with the steady-state measurements, the (intensity weighted) fluorescence lifetimes (0.1 – 0.3 ns) of 5CI in H₂O and TFE are significantly shorter (by at least an order of magnitude) than those in other solvents, which are in the range of 3.0 – 7.1 ns. This finding is, to some extent, surprising, as for indole the fluorescence lifetime in TFE (0.45 ns) is drastically shorter than in H₂O (4.5 ns).³⁰ Barkley and coworkers^{30,31} have shown that both TFE and H₂O can quench the fluorescence of indole via an excited-state proton-transfer process. While we cannot completely rule out the possibility that a solvent-induced proton-transfer event is responsible for the observed fast excited-state decay kinetics of 5CI in H₂O and TFE, the fact that, unlike indole,³⁰ the fluorescence QY and decay kinetics of 5CI do not show any measurable difference between H₂O and D₂O (Figure S1 and Table 1) strongly argues against this scenario. Since both H₂O and TFE can form H-bonds with the nitrile group of 5CI,³² it is possible that their strong quenching effect arises solely from such H-bonding interactions. However, this possibility can also be ruled out as in both MeOH and EtOH, which are able to form such H-bonds, the fluorescence lifetime of 5CI becomes much longer (Table 1). Similarly, the H-bonding interactions between the pyrrole N-H group of 5CI and a solvent molecule, such as H₂O, MeOH, EtOH, and DMSO, are also unlikely to serve as a major nonradiative decay channel as the fluorescence lifetimes of 5CI in those solvents differ significantly (Table 1). It is known that both H₂O and TFE can interact with the indole moiety via another type of H-bonding interactions, i.e. those formed between the –OH group of the solvent and the π -electron cloud of the aromatic ring.^{33–35} In fact, this type of interactions has been suggested to play an important role in the excited-state decay kinetics of indole in TFE.³⁶ Thus, we

tentatively attribute the sub-nanosecond fluorescence decay kinetics of 5CI in H₂O and TFE to such H-bond formations, which increase the nonradiative decay rate of the fluorophore. If this assessment is indeed valid, the much slower fluorescence decay lifetime of 5CI obtained in other protic solvents (i.e., MeOH and EtOH) indicates that the indole ring is solvated mainly by the methyl groups rather than the –OH group, which is consistent with previous studies.^{37,38} In addition, it is noticed that, unlike those obtained in other solvents, the fluorescence decay kinetics of 5CI in H₂O and TFE cannot be satisfactorily described by a single-exponential function (Figure 3). There are two possible interpretations. First, 5CI has a relatively low solubility in both H₂O and TFE; hence the non-single-exponential decay kinetics may reflect the heterogeneity of the solute. The second, and perhaps a more probable interpretation is that this deviation manifests the heterogeneity in the solvent-solute interactions, especially those –OH⋯ π -electron H-bonding interactions.

Finally, unlike that of indole,²⁸ the fluorescence lifetime of 5CI in DMSO is significantly lengthened (i.e., to 7.1 ns) in comparison to those in other solvents, suggesting that Trp_{CN} fluorescence could be used to probe preferential interactions³⁹ between DMSO and Trp sidechains in a protein environment (see below).

As indicated in Figure 3, the fluorescence decay kinetics of Trp_{CN}, in either the free amino acid form or the GW_{CNG} peptide, support the notion that it can be used as a protein hydration probe. While the average fluorescence lifetime of Trp_{CN} obtained in H₂O is slightly increased compared to that of 5CI, its excited-state decay kinetics are still dominated by a fast component (i.e., 0.4–0.5 ns), which is significantly separated from those obtained in other solvents, except TFE (Table 1).

Unlike 5CI, Trp_{CN} exhibits non-single-exponential fluorescence decay kinetics in all the solvents studied. Since Trp shows the same behavior and its double- or multi-exponential fluorescence decay kinetics have been attributed to different sidechain rotamers,¹⁷ we believe that the fluorescence decay kinetics of Trp_{CN} can also be explained by such a rotamer model. Many previous studies have shown that the average fluorescence decay rate of Trp is faster than that of indole under the same solvent conditions, indicating that an additional, nonradiative decay pathway exists due to the presence of a backbone. The current consensus is that this new decay process arises from electron transfer from the indole sidechain to the carbonyl group of adjacent peptide bonds.¹⁶ As shown (Table 1), unlike the trend observed for indole and Trp,²⁸ the average fluorescence lifetime of Trp_{CN} is longer than that of 5CI in the same solvent. More specifically, in most solvents (except H₂O and TFE) the fluorescence decay kinetics of Trp_{CN} and GW_{CNG} consist of two components, with one that is relatively independent of solvent and decays within 2–3 ns, whereas the other, which is slower ($\tau_F > 5.5$ ns) and dominant in most cases, shows a clear dependence on solvent environment. Taken together, these results suggest that the electron-transfer mechanism invoked to explain the fluorescence decay kinetics of Trp is not applicable to Trp_{CN}. Instead, we believe that the fast component arises from a more specific interaction facilitated by differences in geometry between the backbone and a particular sidechain rotamer. While elucidation of the nature of this interaction requires further studies, we hypothesize that it corresponds to a H-bonding-like interaction between the aromatic ring and a backbone amide N–H group. This hypothesis is consistent with the aforementioned

assumption that H₂O quenches the fluorescence of 5CI via H-bonding interactions with the π -electron cloud of the ring. In addition, this model is self-consistent, as for rotamers that cannot engage in such additional interactions due to distance constraints, their fluorescence lifetimes would be longer and depend mostly on the solvent, as observed.

Probing Preferential Interactions with DMSO

To further demonstrate the utility of Trp_{CN} fluorescence as a local solvation reporter, we first applied it to probe the preferential interaction between DMSO and Trp residues within a peptide. The binary mixture of water and DMSO has been extensively studied and used in various applications owing to its non-ideal nature and hence unusual properties.⁴⁰ For example, it has been used as a cryoprotectant, an enzyme activator, and a denaturant.^{41,42} In particular, several studies^{43–45} have indicated that in a binary mixture of water and DMSO preferential solvation of hydrophobic residues, such as Phe and Trp, by DMSO can occur. All of these behaviors can be attributed to the amphiphilic nature of DMSO which allows this solvent to engage in both H-bonding (e.g., with water) and hydrophobic interactions (via methyl groups).⁴⁶ As demonstrated above, the fluorescence QY of Trp_{CN} in DMSO is approximately 24 times greater than its QY in H₂O, making it ideally suited to probe any preferential accumulation of DMSO molecules around its indole ring. Specifically, we measured the fluorescence spectra of a peptide that contains two Trp_{CN} residues (sequence: S-Trp_{CN}-TAENGKAT-Trp_{CN}-K), in a series of DMSO-H₂O mixtures. This peptide (hereafter referred to as 2W_{CN}P) is largely unstructured in aqueous solution according to its CD spectrum (Figure S2), thus allowing the Trp_{CN} sidechains to be solvent accessible.

As shown (Figures 4 and Figure S3), the intensity of the Trp_{CN} fluorescence spectrum of 2W_{CN}P depends strongly on the mole fraction of DMSO (χ_{DMSO}) in the binary mixture, especially in the range of 0.0–0.4. A more quantitative analysis indicates that the relative fluorescence quantum yield of Trp_{CN} in 2W_{CN}P, as measured by the integrated area (I) of the fluorescence spectrum, exhibits a transition (Figure 4) that is similar to that observed in substrate binding kinetics of enzymes. Indeed, this transition (i.e., I vs. χ_{DMSO}) can be satisfactorily described by a modified Hill equation shown below,

$$I = I_{\min} + \frac{(I_{\max} - I_{\min})(a\chi_{\text{DMSO}} + b)}{\left(\frac{k}{\chi_{\text{DMSO}}}\right)^n + 1} \quad (3)$$

where I_{\min} , I_{\max} , k , a , b , and n (the Hill coefficient) are constants. The linear term, $(a\chi_{\text{DMSO}} + b)$, is introduced to account for the slight downward trend of the signal after saturation. As shown in Figure 4, the best fit yields a k value of 0.18, indicating that the fluorescence signal reaches a maximum at a χ_{DMSO} value of 0.36. Interestingly, a previous dielectric relaxation study⁴⁶ indicated that the maximum H-bonding interactions occurring between H₂O and DMSO take place at $\chi_{\text{DMSO}} = 0.33$, leading to formation of H₂O-DMSO-H₂O complexes. Thus, the above result suggests that the fluorescence of Trp_{CN} is able to ‘sense’ this intrinsic property of the binary mixture. In addition, and perhaps more interestingly, the Hill coefficient obtained from the fitting is $n = 3.2$, suggesting that the DMSO binding interaction with the indole ring is highly cooperative. Following the common interpretation of the value of the Hill coefficient,⁴⁷ the above n value suggests that one Trp_{CN} sidechain

can have a maximum of three DMSO binding sites. Hence, from this simple example it becomes evident that Trp_{CN} is not only a useful fluorescence probe of proteins or peptides, but it can also be used to reveal important physical properties of binary solvent systems that contain water.

Probing Peptide-Membrane Interaction

In the second application, we demonstrated that Trp_{CN} fluorescence can be used to probe peptide-membrane interactions. To do so, we measured the static and time-resolved fluorescence properties of a Trp_{CN} mutant of an antimicrobial peptide, mastoparan X, in the presence and absence of a model membrane. Like the parent,⁴⁸ this mutant (sequence: IN-Trp_{CN}-KGIAAMAKKLL), hereafter referred to as MPXW_{CN}, is relatively unstructured in aqueous solution, and folds into an α -helical conformation upon binding to DPC micelles (Figure S4). As shown (Figure 5a and Table 1), in the absence of DPC micelles the Trp_{CN} fluorescence spectrum of MPXW_{CN} is peaked at 391 nm and has a low intensity, which is consistent with an unfolded peptide wherein the Trp_{CN} sidechain is mostly exposed to H₂O. In the presence of DPC micelles, however, the Trp_{CN} fluorescence spectrum of MPXW_{CN} not only is blue-shifted (to 372 nm) but also becomes much more intense, which is characteristic of a Trp_{CN} buried in a hydrophobic environment and, hence, consistent with binding of the peptide to the DPC membranes. Further fluorescence lifetime measurements also corroborate this picture. As shown (Figure 5b and Table 1), the Trp_{CN} fluorescence decay of MPXW_{CN} in H₂O consists of three components, with a sub-nanosecond (i.e., 0.7 ns) component being dominant (~82%). It is clear that this fast decay component corresponds to an ensemble of MPXW_{CN} conformations wherein the Trp_{CN} residue is well hydrated, whereas those slower and minor decay components must arise from conformations wherein the Trp_{CN} sidechain is less exposed to solvent due, for example, to sidechain-sidechain and/or sidechain-backbone interactions. As expected, in the presence of DPC micelles, the Trp_{CN} fluorescence decay of MPXW_{CN}, now dominated by a 7.2 ns component, is similar to those measured for the GW_{CN}G peptide in aprotic solvents (Table 1). Taken together, the above results confirm that both the fluorescence intensity and lifetime of a Trp_{CN} residue can be used to probe various biological binding interactions, as long as its hydration status undergoes a change in response to the binding event in question.

Probing Local Hydration Environment

In the third application, we demonstrated that the high sensitivity of the fluorescence lifetime of Trp_{CN} to H₂O makes it especially useful to differentiate between hydrated and dehydrated environments in a protein. Specifically, we carried out fluorescence lifetime measurements on a double Trp_{CN} mutant of a miniprotein, Trp²-cage.⁴⁹ As suggested by its name, this miniprotein, which was computationally designed based on the miniprotein Trp-cage,⁵⁰ contains two Trp residues, with one (at position 12) being solvent exposed and the other (at position 6) being buried in a hydrophobic cage.⁵⁰ Upon replacing these two Trp residues with Trp_{CN}, we expected that the fluorescence decay kinetics of the resultant double mutant (sequence: NLYIQ-⁶Trp_{CN}-LKDGG-¹²Trp_{CN}-SSGRPPPS), hereafter referred to as TC2W_{CN}, will reflect this difference. As shown (Figure 6 and Table 1), the fluorescence decay kinetics of TC2W_{CN} in H₂O consist of three exponential components with time constants of 0.4, 1.8, 11.0 ns, respectively. The first and very fast component is

similar to the major fluorescence decay component of $\text{GW}_{\text{CN}}\text{G}$ in H_2O , indicating contribution from, and hence detection of, the solvent-exposed Trp_{CN} residue, whereas the slowest component is closer to that of $\text{GW}_{\text{CN}}\text{G}$ in DMSO, representative of the buried and solvent inaccessible Trp_{CN} residue in the protein. Because both the solvent-exposed and buried Trp_{CN} residues can contribute to the 1.8 ns component in the fluorescence decay kinetics of TC2W_{CN} , it is not straightforward to use the relative amplitudes of those three exponentials to directly determine the relative populations of these two differently solvated sidechains. However, if we only consider the other two exponentials (i.e., the 0.4 and 11.0 ns components), which exclusively report the solvent-exposed and buried Trp_{CN} species, and also assume that the radiative rate constant does not change, we can estimate the relative population of the solvent-exposed Trp_{CN} sidechain to be ~58%. As shown (Figure S5, Supporting Information), the CD spectrum of TC2W_{CN} indicates that it is folded. If its stability is assumed to be comparable to that of the wild-type, which has ~10% unfolded population at room temperature,⁴⁹ the solvent-exposed Trp_{CN} should amount to 55%. Thus, the estimate obtained above using the percentages of the 0.4 and 11.0 ns components is reasonable. Taken together, these results, especially the existence of two kinetic components that differ by almost 28 times in their time constants, clearly demonstrate that the fluorescence decay kinetics of Trp_{CN} are sensitive to the presence of H_2O and can be used to differentiate between differently hydrated environments in a protein.

4. CONCLUSIONS

Any spectroscopic study of protein folding, conformational transition and interactions requires a specific probe whose spectroscopic signature would undergo a change in response to a variation in its environment. In practice, an ideal spectroscopic probe is one that can produce a large difference or contrast between signals measured before and after the event of interest. Herein, we demonstrated that the non-natural amino acid, 5-cyanotryptophan, could be used as a sensitive fluorescence probe of proteins. This is because a series of static and time-resolved fluorescence measurements revealed that the fluorescence quantum yield and decay kinetics of 5-cyanotryptophan are sensitively dependent on its hydration status. For example, when fully hydrated its fluorescence quantum yield is approximately 0.01, whereas in a dehydrated environment its quantum yield is increased by at least an order of magnitude. Validation of the potential utility of this non-natural amino acid as a sensitive local protein hydration reporter was demonstrated in three applications, wherein we used it to probe complex formation in a binary mixture, peptide-membrane interactions, and the hydration environments of two tryptophan residues in a miniprotein. Given that 5-cyanotryptophan has also been shown to be a useful site-specific infrared (IR) probe of proteins,⁵¹ we believe that the present work will further expand its utility as a novel spectroscopic probe to study the structure-dynamics-function relationship of proteins.

Supplementary Material

Refer to Web version on PubMed Central for supplementary material.

Acknowledgments

We gratefully acknowledge financial support from the National Institutes of Health (P41GM104605). B.N.M is supported by an NIH Ruth Kirschstein National Research Service Award Predoctoral Fellowship (F31AG046010).

References

1. Royer CA. Probing Protein Folding and Conformational Transitions with Fluorescence. *Chem Rev.* 2006; 106:1769–1784. [PubMed: 16683754]
2. Lakowicz, JR. Principles of Fluorescence Spectroscopy. 3rd. Springer Science & Business Media; New York, NY: 2006.
3. Vivian JT, Callis PR. Mechanisms of Tryptophan Fluorescence Shifts in Proteins. *Biophys J.* 2001; 80:2093–2109. [PubMed: 11325713]
4. Pal SK, Peon J, Zewail AH. Biological Water at the Protein Surface: Dynamical Solvation Probed Directly with Femtosecond Resolution. *Proc Natl Acad Sci U S A.* 2002; 99:1763–1768. [PubMed: 11842218]
5. Yuan T, Weljie AM, Vogel HJ. Tryptophan Fluorescence Quenching by Methionine and Selenomethionine Residues of Calmodulin: Orientation of Peptide and Protein Binding. *Biochemistry.* 1998; 37:3187–3195. [PubMed: 9485473]
6. Qiu WH, Li TP, Zhang LY, Yang Y, Kao YT, Wang LJ, Zhong DP. Ultrafast Quenching of Tryptophan Fluorescence in Proteins: Interresidue and Intrahelical Electron Transfer. *Chem Phys.* 2008; 350:154–164.
7. Alston RW, Lasagna M, Grimsley GR, Scholtz JM, Reinhart GD, Pace CN. Peptide Sequence and Conformation Strongly Influence Tryptophan Fluorescence. *Biophys J.* 2008; 94:2280–2287. [PubMed: 18065477]
8. Lehrer S. Solute Perturbation of Protein Fluorescence. Quenching of the Tryptophyl Fluorescence of Model Compounds and of Lysozyme by Iodide Ion. *Biochemistry.* 1971; 10:3254–3263. [PubMed: 5119250]
9. Eftink MR, Ghiron CA. Fluorescence Quenching Studies with Proteins. *Anal Biochem.* 1981; 114:199–227. [PubMed: 7030122]
10. Zelent B, Ku ba J, Gryczynski I, Johnson ML, Lakowicz JR. Time-Resolved and Steady-State Fluorescence Quenching of N-Acetyl-L-Tryptophanamide by Acrylamide and Iodide. *Biophys Chem.* 1998; 73:53–75. [PubMed: 9697300]
11. Muiño PL, Callis PR. Solvent Effects on the Fluorescence Quenching of Tryptophan by Amides Via Electron Transfer. *Experimental and Computational Studies. J Phys Chem B.* 2009; 113:2572–2577. [PubMed: 18672928]
12. Zhang L, Kao Y-T, Qiu W, Wang L, Zhong D. Femtosecond Studies of Tryptophan Fluorescence Dynamics in Proteins: Local Solvation and Electronic Quenching. *J Phys Chem B.* 2006; 110:18097–18103. [PubMed: 16970418]
13. Chen RF. Fluorescence Quantum Yields of Tryptophan and Tyrosine. *Anal Lett.* 1967; 1:35–42.
14. Petrich JW, Chang MC, McDonald DB, Fleming GR. On the Origin of Nonexponential Fluorescence Decay in Tryptophan and Its Derivatives. *J Am Chem Soc.* 1983; 105:3824–3832.
15. Gudgin E, Lopez-Delgado R, Ware WR. The Tryptophan Fluorescence Lifetime Puzzle. A Study of Decay Times in Aqueous Solution as a Function of pH and Buffer Composition. *Can J Chem.* 1981; 59:1037–1044.
16. Chen Y, Liu B, Yu HT, Barkley MD. The Peptide Bond Quenches Indole Fluorescence. *J Am Chem Soc.* 1996; 118:9271–9278.
17. Adams PD, Chen Y, Ma K, Zagorski MG, Sönnichsen FD, McLaughlin ML, Barkley MD. Intramolecular Quenching of Tryptophan Fluorescence by the Peptide Bond in Cyclic Hexapeptides. *J Am Chem Soc.* 2002; 124:9278–9286. [PubMed: 12149035]
18. Guharay J, Sengupta PK. Characterization of the Fluorescence Emission Properties of 7-Azatriptophan in Reverse Micellar Environments. *Biochem Biophys Res Commun.* 1996; 219:388–392. [PubMed: 8604997]

19. Wong C-Y, Eftink MR. Biosynthetic Incorporation of Tryptophan Analogues into Staphylococcal Nuclease: Effect of 5-Hydroxytryptophan and 7-Azatryptophan on Structure and Stability. *Protein Sci.* 1997; 6:689–697. [PubMed: 9070451]
20. Broos J, Maddalena F, Hesp BH. In Vivo Synthesized Proteins with Monoexponential Fluorescence Decay Kinetics. *J Am Chem Soc.* 2004; 126:22–23. [PubMed: 14709040]
21. Xu JH, Chen BB, Callis P, Muino PL, Rozeboom H, Broos J, Toptygin D, Brand L, Knutson JR. Picosecond Fluorescence Dynamics of Tryptophan and 5-Fluorotryptophan in Monellin: Slow Water-Protein Relaxation Unmasked. *J Phys Chem B.* 2015; 119:4230–4239. [PubMed: 25710196]
22. Talukder P, Chen S, Roy B, Yakovchuk P, Spiering MM, Alam MP, Madathil MM, Bhattacharya C, Benkovic SJ, Hecht SM. Cyanotryptophans as Novel Fluorescent Probes for Studying Protein Conformational Changes and DNA-Protein Interaction. *Biochemistry.* 2015; 54:7457–7469. [PubMed: 26618501]
23. Gosavi PM, Moroz YS, Korendovych IV. Beta-(1-Azulenyl)-L-Alanine - a Functional Probe for Determination of Pka of Histidine Residues. *Chem Commun.* 2015; 51:5347–5350.
24. Jennings P, Jones AC, Mount AR. Fluorescence Properties of Electropolymerised 5-Substituted Indoles in Solution. *J Chem Soc Faraday Trans.* 1998; 94:3619–3624.
25. Hill PA, Wei Q, Troxler T, Dmochowski IJ. Substituent Effects on Xenon Binding Affinity and Solution Behavior of Water-Soluble Cryptophanes. *J Am Chem Soc.* 2009; 131:3069–3077. [PubMed: 19239271]
26. Oeltermann O, Brand C, Engels B, Tatchen J, Schmitt M. The Structure of 5-Cyanoindole in the Ground and the Lowest Electronically Excited Singlet States, Deduced from Rotationally Resolved Electronic Spectroscopy and Ab Initio Theory. *Phys Chem Chem Phys.* 2012; 14:10266–10270. [PubMed: 22729279]
27. Kirby EP, Steiner RF. Influence of Solvent and Temperature Upon the Fluorescence of Indole Derivatives. *J Phys Chem.* 1970; 74:4480–4490.
28. Chen Y, Gai F, Petrich JW. Single-Exponential Fluorescence Decay of the Nonnatural Amino Acid 7-Azatryptophan and the Nonexponential Fluorescence Decay of Tryptophan in Water. *J Phys Chem.* 1994; 98:2203–2209.
29. Waegle MM, Tucker MJ, Gai F. 5-Cyanotryptophan as an Infrared Probe of Local Hydration Status of Proteins. *Chem Phys Lett.* 2009; 478:249–253. [PubMed: 20161057]
30. Chen Y, Liu B, Barkley MD. Trifluoroethanol Quenches Indole Fluorescence by Excited-State Proton Transfer. *J Am Chem Soc.* 1995; 117:5608–5609.
31. Yu HT, Colucci WJ, McLaughlin ML, Barkley MD. Fluorescence Quenching in Indoles by Excited-State Proton Transfer. *J Am Chem Soc.* 1992; 114:8449–8454.
32. Zhang W, Markiewicz BN, Doerksen RS, Smith AB III, Gai F. C≡N Stretching Vibration of 5-Cyanotryptophan as an Infrared Probe of Protein Local Environment: What Determines Its Frequency? *Phys Chem Chem Phys.* 2015; 1039/C1035CP04413H
33. Zhang RB, Somers KRF, Kryachko ES, Nguyen MT, Zeegers-Huyskens T, Ceulemans A. Hydrogen Bonding to Pi-Systems of Indole and 1-Methylindole: Is There Any OH...Phenyl Bond? *J Phys Chem A.* 2005; 109:8028–8034. [PubMed: 16834185]
34. Othon CM, Kwon O-H, Lin MM, Zewail AH. Solvation in Protein (Un)Folding of Melittin Tetramer–Monomer Transition. *Proc Natl Acad Sci U S A.* 2009; 106:12593–12598. [PubMed: 19622745]
35. Johnston AJ, Zhang Y, Busch S, Pardo LC, Imberti S, McLain SE. Amphipathic Solvation of Indole: Implications for the Role of Tryptophan in Membrane Proteins. *J Phys Chem B.* 2015; 119:5979–5987. [PubMed: 25893741]
36. Muñoz, MaA; Carmona, C.; Balón, M. The Ground and Singlet Excited-State Hydrogen-Bonding Interactions of N-Methylindole with Trifluoroethanol in N-Hexane: A Model to Explain the Anomalous Fluorescence of Indole in Polar Protic Solvents. *Chem Phys Lett.* 2004; 393:217–221.
37. Gervasio FL, Chelli R, Marchi M, Procacci P, Schettino V. Determination of the Potential of Mean Force of Aromatic Amino Acid Complexes in Various Solvents Using Molecular Dynamics Simulations: The Case of the Tryptophan–Histidine Pair. *J Phys Chem B.* 2001; 105:7835–7846.

38. Albani JR. Origin of Tryptophan Fluorescence Lifetimes Part 1. Fluorescence Lifetimes Origin of Tryptophan Free in Solution. *J Fluoresc.* 2014; 24:93–104. [PubMed: 23912963]
39. Roy S, Bagchi B. Solvation Dynamics of Tryptophan in Water-Dimethyl Sulfoxide Binary Mixture: In Search of Molecular Origin of Composition Dependent Multiple Anomalies. *J Chem Phys.* 2013; 139:034308. [PubMed: 23883028]
40. Kiefer J, Noack K, Kirchner B. Hydrogen Bonding in Mixtures of Dimethyl Sulfoxide and Cosolvents. *Curr Phys Chem.* 2011; 1:340–351.
41. Kaatze U, Pottel R, Schäfer M. Dielectric Spectrum of Dimethyl Sulfoxide/Water Mixtures as a Function of Composition. *J Phys Chem.* 1989; 93:5623–5627.
42. Johnson ME, Malardier-Jugroot C, Head-Gordon T. Effects of Co-Solvents on Peptide Hydration Water Structure and Dynamics. *Phys Chem Chem Phys.* 2010; 12:393–405. [PubMed: 20023817]
43. Arakawa T, Kita Y, Timasheff SN. Protein Precipitation and Denaturation by Dimethyl Sulfoxide. *Biophys Chem.* 2007; 131:62–70. [PubMed: 17904724]
44. Roy S, Jana B, Bagchi B. Dimethyl Sulfoxide Induced Structural Transformations and Non-Monotonic Concentration Dependence of Conformational Fluctuation around Active Site of Lysozyme. *J Chem Phys.* 2012; 136:115103. [PubMed: 22443797]
45. Gasyimov OK, Abduragimov AR, Glasgow BJ. Site-Directed Circular Dichroism of Proteins: 11b Bands of Trp Resolve Position-Specific Features in Tear Lipocalin. *Anal Biochem.* 2008; 374:386–395. [PubMed: 18047823]
46. Lu Z, Manias E, Macdonald DD, Lanagan M. Dielectric Relaxation in Dimethyl Sulfoxide/Water Mixtures Studied by Microwave Dielectric Relaxation Spectroscopy. *J Phys Chem A.* 2009; 113:12207–12214. [PubMed: 19817400]
47. Pignataro, B. Ideas in Chemistry and Molecular Sciences: Advances in Nanotechnology, Materials and Devices. Vol. 1. WILEY-VCH Verlag GmbH & Co. KGaA; Weinheim: 2010. p. 332
48. Tucker MJ, Oyola R, Gai F. Conformational Distribution of a 14-Residue Peptide in Solution: A Fluorescence Resonance Energy Transfer Study. *J Phys Chem B.* 2005; 109:4788–4795. [PubMed: 16851563]
49. Bunagan MR, Yang X, Saven JG, Gai F. Ultrafast Folding of a Computationally Designed Trp-Cage Mutant: Trp(2)-Cage. *J Phys Chem B.* 2006; 110:3759–3763. [PubMed: 16494434]
50. Barua B, Lin JC, Williams VD, Kummner P, Neidigh JW, Andersen NH. The Trp-Cage: Optimizing the Stability of a Globular Miniprotein. *Protein Eng Des Sel.* 2008; 21:171–185. [PubMed: 18203802]
51. Ma J, Pazos IM, Zhang W, Culik RM, Gai F. Site-Specific Infrared Probes of Proteins. *Annu Rev Phys Chem.* 2015; 66:357–377. [PubMed: 25580624]

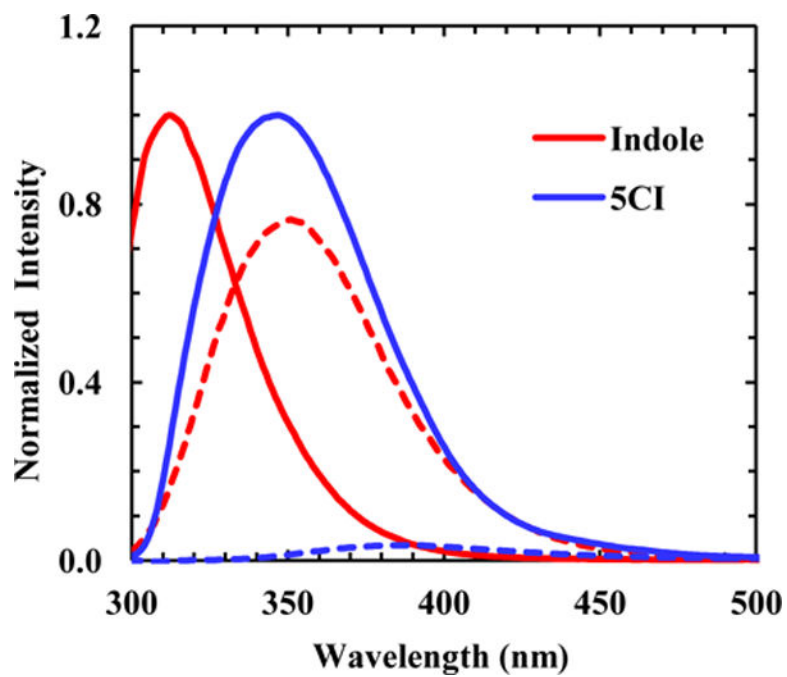


Figure 1. Normalized fluorescence spectra of indole and 5CI obtained in 1,4-dioxane (solid lines) and H₂O (dashed lines), as indicated.

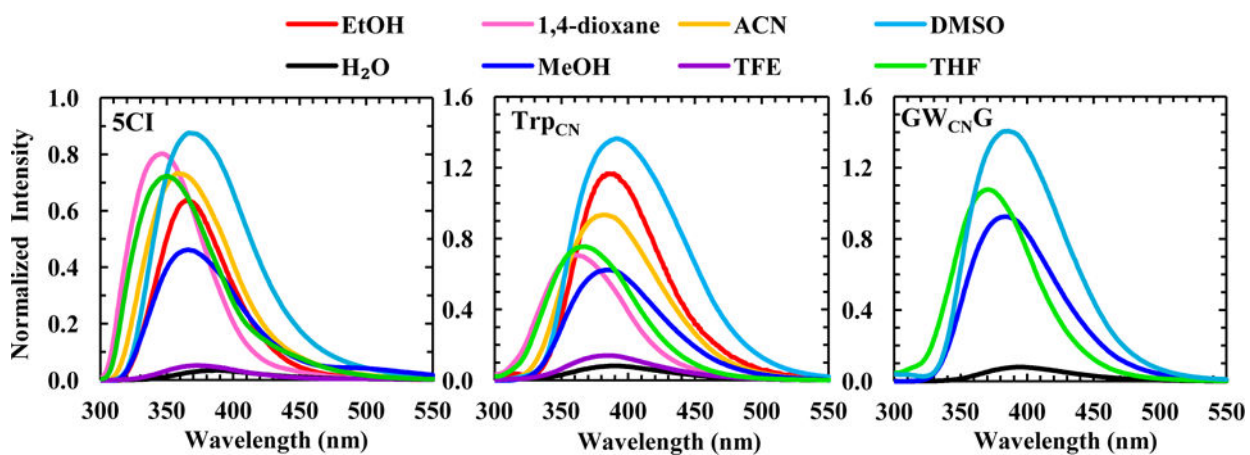


Figure 2.

Fluorescence spectra of 5CI, Trp_{CN}, and GW_{CN}G in different solvents, normalized against the fluorescence spectrum of NATA obtained in H₂O. In each case, the normalization factor was calculated based on the integrated areas of the corresponding fluorescence spectra.

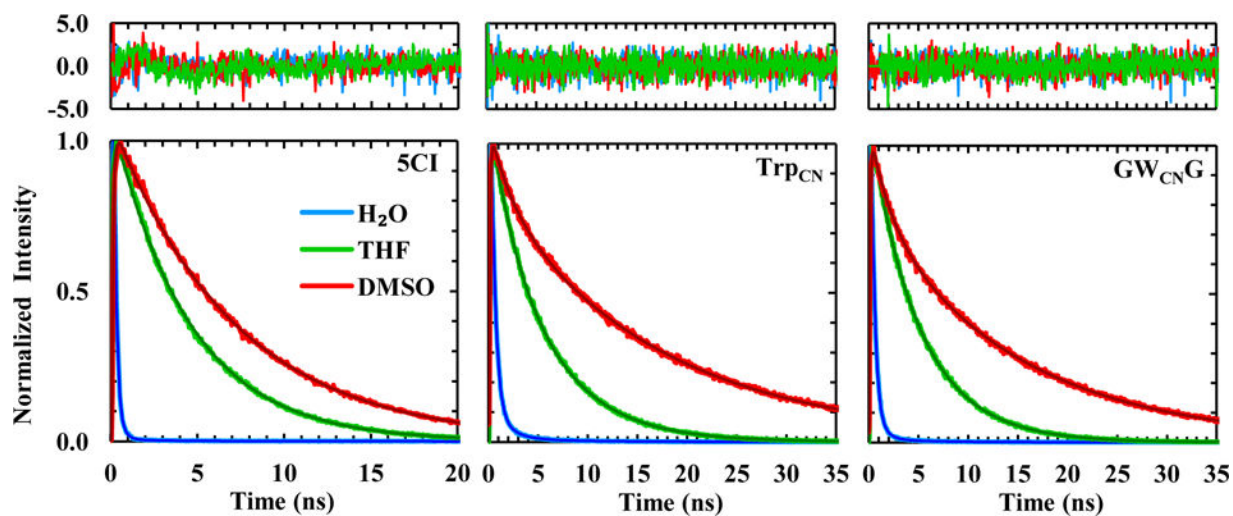


Figure 3.

Fluorescence decay kinetics of 5CI, Trp_{CN}, and GW_{CNG} in three representative solvents, as indicated. In each case, the smooth line corresponds to a fit of the kinetics to either a single- or double-exponential function and the resulting fitting parameters are listed in Table 1. Shown in the top panel are the residuals of the fits of the unnormalized data.

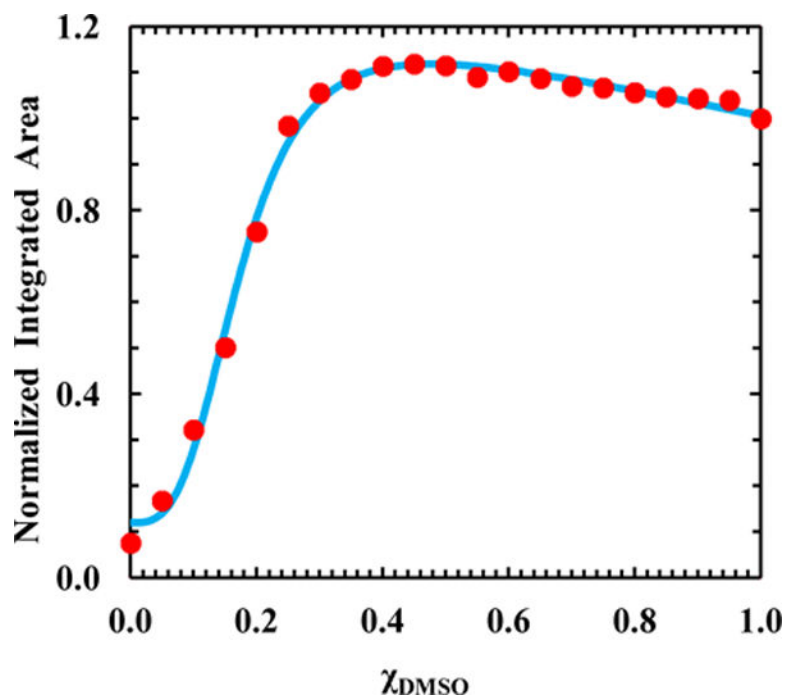


Figure 4. Integrated area of the Trp_{CN} fluorescence spectrum of 2W_{CN}P versus the mole fraction of DMSO (χ_{DMSO}) in the H₂O-DMSO binary solvent. These data have been normalized such that the value obtained in pure DMSO is 1.0. The smooth line is the best fit of the data to a modified Hill equation (i.e., Eq. 3) with the following parameters: $I_{\text{min}} = 0.11 \pm 0.02$, $I_{\text{max}} = 1.10 \pm 0.01$, $k = 0.18 \pm 0.01$, $n = 3.20 \pm 0.29$, $a = -0.30 \pm .01$, and $b = 1.20 \pm 0.01$.

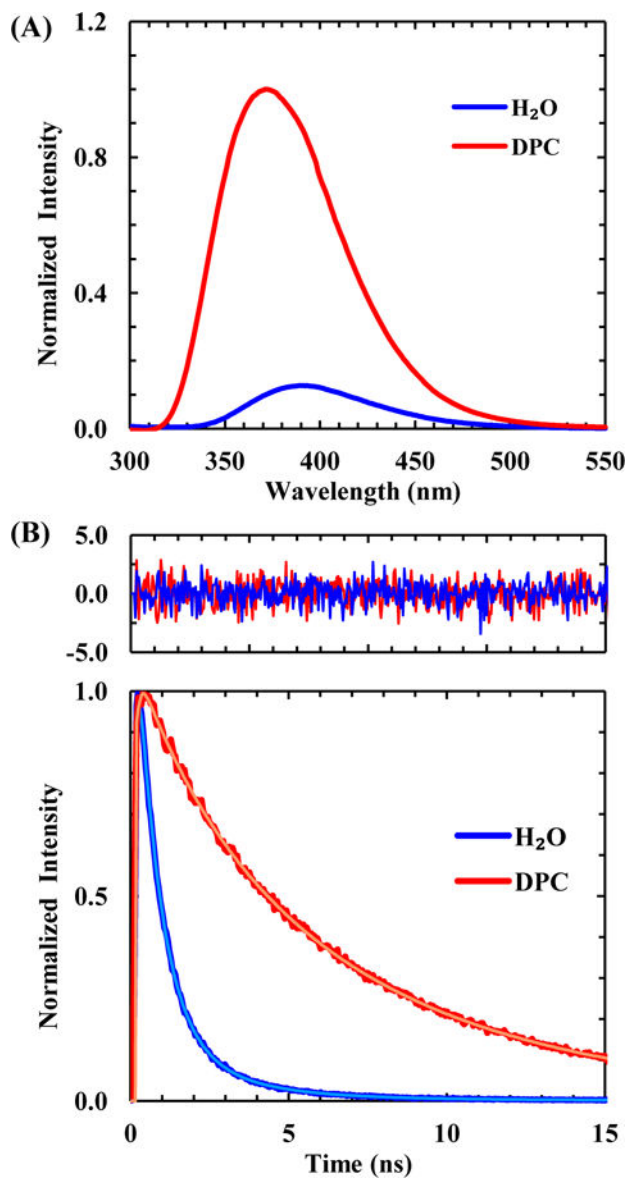


Figure 5.

(A) Normalized fluorescence spectra of MPXW_{CN} obtained in H₂O and DPC micelles, as indicated. The lipid to peptide ratio was 1:70 with a final peptide concentration of 40 μ M. (B) Normalized Trp_{CN} fluorescence decay kinetics of MPXW_{CN} in H₂O and DPC micelles, as indicated. In each case, the smooth line is the best fit of the data to a triple-exponential function and the resulting fitting parameters are listed in Table 1. Shown in the top panel are the residuals of the fits of the unnormalized data.

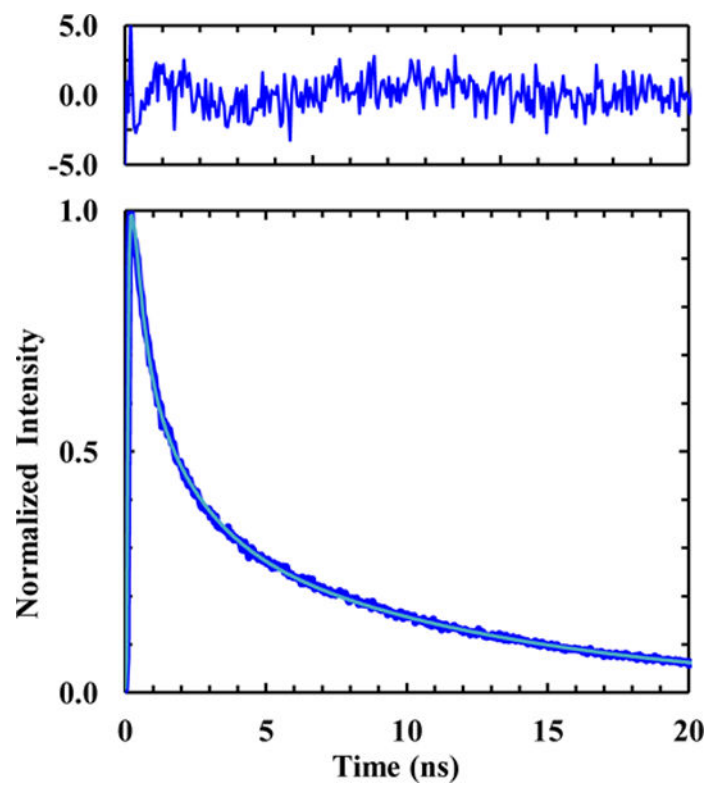


Figure 6. Normalized Trp_{CN} fluorescence decay kinetics of TC2W_{CN} in H₂O. The smooth line is the best fit of the data to a triple-exponential function and the resulting fitting parameters are listed in Table 1. Shown in the top panel are the residuals of the fit of the unnormalized data.

Table 1

Summary of results obtained from all static and time-resolved fluorescence measurements. QY was determined using the value of NATA as a standard. τ_{ave} corresponds to the intensity weighted average fluorescence lifetime.

	Solvent	λ_{max} (nm)	# exp	%	τ_F (ns)	τ_{ave} (ns)	QY	χ^2
5CI	H ₂ O	387	2	91	0.10	0.3	0.005	1.19
				9	0.3			
	D ₂ O	385	2	88	0.13	0.4	0.002	0.99
				12	0.30			
	TFE	373	2	97	<0.1	0.1	0.007	1.05
				3	0.3			
	MeOH	366	1	100	2.9	2.9	0.06	1.04
	EtOH	366	1	100	4.3	4.3	0.09	1.14
	ACN	358	1	100	4.4	4.4	0.10	1.17
	1,4-dioxane	347	1	100	4.2	4.2	0.13	1.04
TrpCN	THF	345	1	100	4.4	4.4	0.11	1.15
	DMSO	367	1	100	7.1	7.1	0.15	1.18
	H ₂ O	391	2	91	0.4	1.4	0.01	0.97
				9	1.6			
	TFE	386	3	53	<0.1	1.1	0.02	1.10
				44	0.7			
				3	2.8			
	MeOH	384	2	10	1.8	5.4	0.09	1.09
				90	5.6			
	EtOH	386	2	18	2.3	6.5	0.17	1.20
			82	6.8				
1,4-dioxane	ACN	381	2	67	3.1	5.5	0.13	1.07
				33	7.5			
				25	3.4	5.6	0.11	1.11
				75	6.0			
	THF	368	2	18	2.5	5.6	0.12	1.07
				82	5.9			

Solvent	λ_{max} (nm)	# exp	%	τ_{F} (ns)	τ_{ave} (ns)	QY	χ^2
DMSO	391	2	21	2.1	16.1	0.24	1.06
			79	16.5			
GW_{CN}G							
H ₂ O	394	2	96	0.5	0.8	0.01	0.93
			4	2.1			
MeOH	383	2	24	0.8	5.7	0.13	1.16
			76	6.0			
THF	371	2	17	3.0	5.3	0.14	1.04
			83	5.6			
DMSO	386	2	26	2.0	13.9	0.24	1.13
			74	14.5			
MPXW_{CN}							
H ₂ O	391	3	82	0.7	1.6	0.02	0.94
			17	2.0			
			1	6.1			
MPXW_{CN}							
DPC	372	2	24	2.4	6.7	0.18	1.08
			76	7.2			
TC2W_{CN}							
H ₂ O	387	3	40	0.4	9.2	0.06	1.18
			31	1.8			
			29	11.0			
NATA							
H ₂ O/pH 7	358	1	100	3.0	3.0	0.14*	1.03

* Value adopted from ref. 2